

Near Threshold Photoproduction of η Mesons off the Proton

B. Krusche,^{1,*} J. Ahrens,² G. Anton,⁴ R. Beck,² M. Fuchs,¹ A. R. Gabler,¹ F. Härter,² S. Hall,³ P. Harty,³ S. Hlavac,⁵
 D. MacGregor,³ C. McGeorge,³ V. Metag,¹ R. Owens,³ J. Peise,² M. Röbig-Landau,¹ A. Schubert,⁵ R. S. Simon,⁵
 H. Ströher,¹ and V. Tries¹

¹*II. Physikalisches Institut, Universität Giessen, D-35392 Giessen, Germany*

²*Institut für Kernphysik, Johannes-Gutenberg-Universität Mainz, D-55099 Mainz, Germany*

³*Kelvin Laboratory, University of Glasgow, United Kingdom*

⁴*Physikalisches Institut, Universität Bonn, D-53115 Bonn, Germany*

⁵*Gesellschaft für Schwerionenforschung, D-64220 Darmstadt, Germany*

(Received 1 December 1994)

We have measured precise total and differential cross sections for the reaction $\gamma p \rightarrow p\eta$ from threshold to 790 MeV at the MAMI accelerator in Mainz with the neutral meson spectrometer TAPS. Resonance parameters of the $S_{11}(1535)$ resonance and the electromagnetic coupling $\gamma p \rightarrow S_{11}$ have been extracted from the data. Contributions from the $D_{13}(1520)$ resonance to η photoproduction in the threshold region have been identified for the first time via interference terms in the angular distributions.

PACS numbers: 13.60.Le, 14.20.Gk, 14.40.Aq, 25.20.Lj

Excitation energies and quantum numbers of the low lying nucleon resonances are well known. Properties like mass, spin, and parity alone, however, do not offer stringent tests of hadron models. Much more crucial tests are provided by the investigation of transitions between the states, which reflect their internal structure. The dominant decay channel of nucleon resonances is the hadronic decay via meson emission. Photoproduction of mesons, which carries information on strong and electromagnetic decay properties, therefore provides a very valuable tool for their study. Because of their hadronic decay modes nucleon resonances have large, overlapping widths. This makes it difficult to study individual states, in particular, those which are only weakly excited. This problem can be partly overcome by looking at decay channels which, due to selection rules, are specific to certain resonances. The isoscalar η meson is an obvious candidate because, due to isospin conservation, only the N^* ($I = 1/2$) resonances decay into the ηN channel.

Three resonances may contribute to η photoproduction on the proton in the threshold region, namely, the $P_{11}(1440)$, the $D_{13}(1520)$, and the $S_{11}(1535)$ resonance. Furthermore, contributions from nucleon Born terms and vector meson exchange must be considered.

Recently, renewed interest in this reaction has prompted major advances in its theoretical treatment. Benmerrouche and Mukhopadhyay [1] developed an effective Lagrangian approach, which for the first time treated resonances and background terms on an equal footing. In a different approach [2,3] a coupled channel model is used to make predictions for the resonance contributions from an analysis of related reactions. An unsolved problem common to both models is the very poor knowledge about the ηNN vertex. As already pointed out in [1], not only the coupling constant but also the coupling structure of the Born terms is unknown. Tiator *et al.* [3] have recently shown that differ-

ential cross sections are rather sensitive to the assumptions about this vertex, and, therefore, precise $\gamma p \rightarrow p\eta$ data might clarify the coupling structure.

Previous attempts to extract the interesting physical observables were severely limited by the lack of precise data. Altogether only some 20 data points with rather large error bars have been reported in the energy range below 800 MeV [4]. With the advent of high duty factor electron accelerators, providing tagged photon beams of excellent quality allied to the development of powerful detector systems, the opportunity for a new generation of very precise experiments has emerged.

In this paper we present the results of a precise measurement of η photoproduction from threshold at $E_\gamma \approx 707$ MeV ($\sqrt{s} \approx 1485$ MeV) to 790 MeV ($\sqrt{s} \approx 1537$ MeV) using the MAMI accelerator [5] in Mainz with the Glasgow tagged photon facility [6] and the neutral meson spectrometer TAPS [7].

The 855 MeV cw electron beam was used to generate quasimonochromatic photons by means of bremsstrahlung tagging. The η mesons, produced in a 5 cm long liquid hydrogen target, were detected via their γ -decay channels in the TAPS detector system. The spectrometer consists of hexagonally shaped BaF₂ modules of 25 cm length and 5.9 cm diameter, 64 of which are arranged in an 8×8 matrix to form each TAPS block. Five blocks were placed in a horizontal plane around the target at a distance of 55 cm and at angles of $\pm 38^\circ$, $\pm 88^\circ$, and $+133^\circ$ with respect to the beam axis. With the exception of the 133° block, all BaF₂ modules were equipped with individual plastic veto detectors. In this configuration the spectrometer was sensitive to the decays of η mesons emitted at any angle in the 0° – 180° range for all photon energies studied. The photon response of the spectrometer was investigated by moving one block into the photon beam.

Details of the energy calibration and the measured response are given in Ref. [8].

Background from particles was completely removed with the aid of the veto detectors, pulse shape analysis (PSA), and time-of-flight (TOF) analysis [9]. Events from the 2γ decay of the η meson were identified with a standard invariant mass analysis using $m_{\text{inv}} = [2E_{\gamma_1}E_{\gamma_2}(1 - \cos \Phi_{\gamma\gamma})]^{1/2}$, where E_{γ_1} , E_{γ_2} are the photon energies and $\Phi_{\gamma\gamma}$ is the opening angle between the photons. A resolution of ≈ 45 MeV FWHM was achieved, and the invariant mass spectrum was practically free of background in the region of the η peak [10]. The unwanted residual η events due to random coincidences between TAPS and the tagging spectrometer and η production in the target windows ($2 \times 60 \mu\text{m}$ Kapton) were strongly suppressed by exploiting the kinematical overdetermination of the reaction by means of missing energy cuts [9]. After subtraction of the remaining random background ($<10\%$) and the empty target background ($<1.5\%$) the η yield below threshold was consistent with zero and its fluctuations were small compared to the yield above threshold.

Because of the modest solid angle coverage of TAPS ($\approx 23\%$ of 4π) the count rates for sixfold and fivefold coincidences from the $\eta \rightarrow 3\pi^0 \rightarrow 6\gamma$ decay were too low to provide comparable accuracy to the 2γ decay. However, threefold and fourfold coincidences from the $\eta \rightarrow 3\pi^0$ channel were used to determine the total cross section. Background from the $\gamma p \rightarrow p\pi^0\pi^0$ reaction was suppressed by kinematical constraints in the case of fourfold coincidences [10], but for threefold coincidences it must be determined by fitting below the η -production threshold. The threefold yield was therefore used only close to threshold where this background contribution can be linearly extrapolated.

The normalization of the cross section was obtained from the target thickness (0.4 g/cm^2), the intensity of the photon beam, the detection efficiency of TAPS, and the branching ratios of the η -meson decays. The photon intensity was determined by counting the deflected electrons in the tagging spectrometer and measuring the tagging efficiency (i.e., the fraction of the correlated photons which pass through the photon collimator) by moving a lead glass detector into the photon beam at reduced intensity (approximately twice a day). Small drifts of the tagging efficiency were monitored by measuring the large π^0 yield from the $\gamma p \rightarrow p\pi^0$ reaction. The angle and energy dependent detection efficiency of TAPS was modeled with Monte Carlo simulations, carried out with the GEANT3 code [11]. Excellent agreement was found between the measured and simulated spectra [9,10].

Figure 1 shows the total cross section for the $\gamma p \rightarrow p\eta$ reaction as derived from the different η -decay channels. The good agreement indicates that systematic errors in the η identification in TAPS and in the simulation of the detection efficiency must be very small. Their size was investigated by analyzing the data with different cut

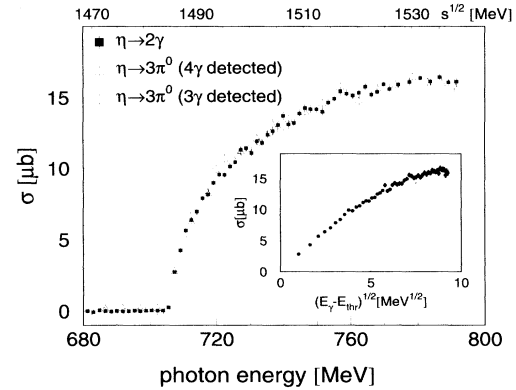


FIG. 1. Total cross section of the $\gamma p \rightarrow p\eta$ reaction. The results from the different decay channels are indicated. The inset shows the almost linear behavior near threshold as a function of the square root of the energy above the threshold.

conditions on TOF, PSA, and invariant mass spectra. In total we estimate a systematic error of 4% (2% analysis cuts, 2% Monte Carlo simulations, 1.5% effective target thickness, 1.3% η decay branching ratios, and 1% tagging efficiency). The statistical errors are on the order of 2%–3%.

The differential cross sections were obtained from the analysis of the $\eta \rightarrow 2\gamma$ decay alone. They are displayed, averaged over reasonable energy bins, in Fig. 2. The resolution (FWHM) of the c.m. polar angle was between 10° and 25° with the exception of the lowest energy bin, in which it rose to 40° . The acceptance of the c.m. polar angle was deduced from the Monte Carlo simulations for each bin of incident photon energies (i.e., in steps of ≈ 1.6 MeV). It was verified that the application of the same procedure to the simultaneously measured $\gamma p \rightarrow p\pi^0$ reaction recovers its well-known angular distributions. In order to separate s -, p -, and d -wave components the distributions have been fitted using the usual ansatz,

$$\frac{d\sigma}{d\Omega} = \frac{q_\eta^*}{k^*} [A + B \cos(\Theta^*) + C \cos^2(\Theta^*)], \quad (1)$$

where q_η^* , k^* are the c.m. momenta of the η meson and the incident photon, respectively, and Θ^* is the c.m. polar angle of the η . Within the statistical accuracy higher order terms are consistent with zero. The results of the fits are also displayed in Fig. 2.

One of the most interesting questions concerns the contributions of the different resonances, and this is revealed by the threshold behavior of the cross section and the angular distribution. The energy dependence of the total cross section is given by $(E_\gamma - E_{\text{thr}})^{l+1/2}$, where E_{thr} is the threshold energy and l is the order of the dominant multipole. The angular distributions of the E_{0+} multipole (S_{11}) and the M_{1-} multipole (P_{11}) are isotropic, although if both contribute an additional interference term proportional to $\cos(\Theta^*)$ appears. However, the E_{2-} and M_{2-} multipoles from the D_{13} resonance involve $\cos^2(\Theta^*)$ terms.

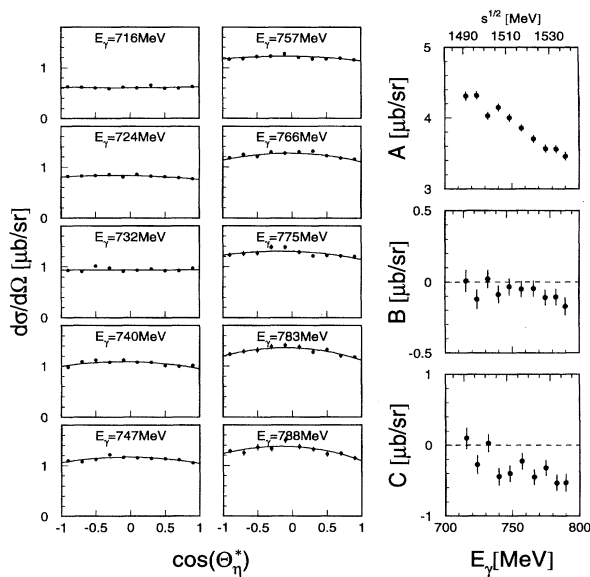


FIG. 2. Differential cross sections for the $\gamma p \rightarrow p \eta$ reaction in the c.m. system for different energy bins. The lines are fits according to Eq. (1). The fitted coefficients A , B , C of the angular distributions are displayed at the right hand side.

The energy dependence of the total cross section (see Fig. 1) clearly exhibits a $(E_\gamma - E_{\text{thr}})^{1/2}$ threshold behavior typical of the s -wave E_{0^+} multipole, and the angular distributions are completely dominated by the constant term. Together these underline the strong dominance of the S_{11} resonance, which was already pointed out in Refs. [1,3,12]. In the absence of significant contributions from other multipoles, the E_{0^+} amplitude is related to the total cross section via

$$|E_{0^+}(W)| = \left(\frac{1}{4\pi} \frac{k^*}{q_\eta^*} \sigma(W) \right)^{1/2}. \quad (2)$$

In Fig. 3 this phase space reduced cross section has been fitted with a Breit-Wigner curve

$$\frac{k^*}{q_\eta^*} \sigma(W) = \frac{A W_R^2 \Gamma_R^2}{(W_R^2 - W^2)^2 + W_R^2 \Gamma(W)^2}, \quad (3)$$

where W_R and Γ_R are the resonance position and width, respectively, and the energy dependent width

$$\Gamma(W) = \Gamma_R \left(b_\eta \frac{q_\eta^*}{q_{\eta R}^*} + b_\pi \frac{q_\pi^*}{q_{\pi R}^*} + b_{\pi\pi} \right) \quad (4)$$

is needed because the resonance is located very close to the η -production threshold. This width is parametrized in terms of the η and π c.m. momenta q_η^* , q_π^* , the respective momenta at resonance and the S_{11} decay branching ratios b_η , b_π , and $b_{\pi\pi}$. The branching ratios are not well known ($b_\eta = 0.3 - 0.55$, $b_\pi = 0.35 - 0.55$, $b_{\pi\pi} \leq 0.1$ [13]). We have, therefore, performed three different fits, spanning the parameter range. The results are summarized in Table I. The χ^2 of the fits are almost identical and do not restrict the branching ratios. Taking into account this uncertainty, the best resonance parameters are $W_R =$

(1544 ± 13) MeV and $\Gamma_R = (200 \pm 40)$ MeV. The corresponding Breit-Wigner curve is compared to our data in Fig. 3 together with the curve corresponding to the Particle Data Group (PDG) values [13].

From the fit we extrapolate an $|E_{0^+}|$ amplitude of $(16 \pm 1) \times 10^{-3}/m_{\pi^+}$ at threshold. The corresponding phase depends strongly on the S_{11} decay branching ratios as indicated in Table I and in the inset of Fig. 3. However, even taking into account this uncertainty, the imaginary part seems to be somewhat larger than the coupled channel value of $\approx 6 \times 10^{-3}/m_{\pi^+}$ [3], while the real part is more consistent with the values given in Ref. [1] ($\approx 9 \times 10^{-3}/m_{\pi^+}$), and in Ref. [3] ($\approx 11 \times 10^{-3}/m_{\pi^+}$).

The electromagnetic helicity amplitude $A_{1/2}$ of the $\gamma p \rightarrow S_{11}$ transition, which is of great interest for hadron models, is related to the E_{0^+} multipole via [13]

$$A_{1/2} = \left[(2J + 1) \pi \frac{q_\eta^*}{k^*} \frac{W_R}{m_p} \frac{\Gamma_R}{\Gamma_\eta} \right]^{-1/2} \text{Im}[E_{0^+}(W_R)]. \quad (5)$$

If contributions other than S_{11} are neglected this reduces to

$$A_{1/2} = \left(\frac{W_R}{2m_p} \right)^{1/2} \left(\frac{\Gamma_R}{b_\eta} \right)^{1/2} \sigma(W_R)^{1/2}. \quad (6)$$

The uncertainty of the first term is less than 1%, and contributions to the total cross section from channels other than the S_{11} resonance are estimated to be below 10% [1,3]. Consequently, the major uncertainty is produced by the term Γ_R/b_η , in which both the width and the branching ratio have errors at the 20% level. The value obtained is $A_{1/2} = (125 \pm 25)$. Estimates of this amplitude from quark models range from 54 to 162 [1]. Experimental results from pion photoproduction are clustered between 50 and 80 [13], while the only results reported until now from η photoproduction are (95 ± 11) (error does not include uncertainty of Γ_R , b_η) [1] and 133^{+55}_{-39} [14] (all in units of $10^{-3} \text{ GeV}^{1/2}$). The results from pion photoproduction, where the S_{11} resonance

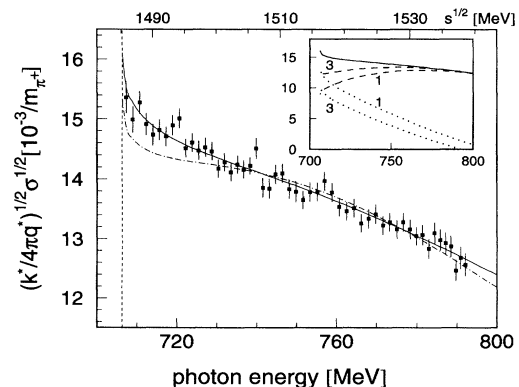


FIG. 3. This figure displays the reduced cross section versus photon energy. The full line is our Breit-Wigner fit, the dash-dotted line the Breit-Wigner curve obtained from the PDG resonance parameters. The inset shows the decomposition of the fit into the imaginary (dashed) and real (dotted) part for the fits 1 and 3 (see Table I).

TABLE I. S_{11} parameters obtained from the Breit-Wigner fits. Fit 1 corresponds to $b_\eta = 0.55$, $b_\pi = 0.35$, fit 2 to $b_\eta = 0.45$, $b_\pi = 0.45$, and fit 3 to $b_\eta = 0.35$, $b_\pi = 0.55$. Also given are the $|E_{0^+}|$ value at threshold and the electromagnetic coupling $A_{1/2}$ extracted from the fits.

	Fit 1	Fit 2	Fit 3	PDG ^a
W_R [MeV]	1549 ± 8	1544 ± 8	1539 ± 8	1520–1555 (1535)
Γ_R [MeV]	202 ± 35	203 ± 35	208 ± 35	100–250 (150)
$ E_{0^+} ^b$	16.14	16.08	16.05	
$\text{Re}(E_{0^+})^b$	13.4	12.0	10.3	
$\text{Im}(E_{0^+})^b$	9.0	10.7	12.3	
$A_{1/2}^c$	110	125	140	29–95 (68 ± 10)

^aFrom Ref. [13], recommended values in parentheses.

^bIn units of $[10^{-3}/m_{\pi^+}]$.

^cIn units of $[10^{-3} \text{ GeV}^{1/2}]$.

contributes only weakly, seem not to be consistent with the $\gamma p \rightarrow p\eta$ data. The most recent PDG recommended value of (68 ± 10) [13], which is mostly based on the pion data but already includes the comparably large value of Ref. [1], is clearly lower than our result.

Finally, the contribution of other resonances was examined. The dominance of the S_{11} resonance allows us to expand the cross section in terms proportional to the E_{0^+} multipole [3]:

$$\frac{d\sigma}{d\Omega} = \frac{q_\eta^*}{k^*} \{ E_{0^+}^{2*} - \text{Re}[E_{0^+}^*(E_{2^-} - 3M_{2^-}) - 2\text{Re}[E_{0^+}^*(3E_{1^+} + M_{1^+} - M_{1^-})] \cos(\Theta^*) + 3\text{Re}[E_{0^+}^*(E_{2^-} - 3M_{2^-})] \cos^2(\Theta^*) \}. \quad (7)$$

Contributions from the P_{11} resonance would enter into the $\cos(\Theta^*)$ term and those from the D_{13} resonance into the $\cos^2(\Theta^*)$ term. However, additional contributions from vector meson exchange and nucleon Born terms are also expected in the $\cos(\Theta^*)$ term, which experimentally is found to be very small (less than 1% of the constant term), so that no significant contribution from the P_{11} resonance can be identified.

In the case of the $\cos^2(\Theta^*)$ term, which is dominated by the D_{13} resonance, the value is significantly different from zero ($\approx 10\%$ of the constant term). Thus for the first time, the contribution from this resonance has been experimentally established. This was possible because its influence on the angular distribution is strongly enhanced by the structure of the interference term [see Eq. (7)], whereas its contribution to the total cross section is almost negligible. The relative sign of the interference term and its absolute magnitude are in good agreement with coupled channel predictions [3].

In conclusion, we have obtained very precise results for η photoproduction on the proton in the threshold region. The data clearly show the strong dominance of the S_{11} resonance. Resonance parameters and the electromagnetic coupling to the nucleon ground state have been extracted. For the first time contributions from the $D_{13}(1520)$ resonance have been identified via interference terms.

We wish to acknowledge the outstanding support of the accelerator group of MAMI, as well as many other scientists and technicians of the Institute für Kernphysik at the University of Mainz. We are very grateful to L. Tiator, N. Mukhopadhyay, and C. Wilkins for many stimulating discussions. This work was supported by Deutsche Forschungsgemeinschaft (SFB 201), Bundesministerium für Forschung und Technologie (BMFT, Contract No. 06 GI 174 I), Gesellschaft für Schwerionenforschung (GSI, Contract GI Met K), and the U.K. Science and Engineering Research Council.

*The cross section data are available via electronic mail request at BERND@PIGGY.PHYSIK.UNI-GIESSEN.DE

- [1] M. Benmerrouche and Nimai C. Mukhopadhyay, Phys. Rev. Lett. **67**, 1070 (1991), and references therein.
- [2] C. Bennhold *et al.*, Nucl. Phys. **A530**, 625 (1991).
- [3] L. Tiator *et al.*, Nucl. Phys. **A580**, 455 (1994).
- [4] R. Preprost *et al.*, Phys. Rev. Lett. **18**, 82 (1967); C. Bacci *et al.*, *ibid.* **20**, 573 (1968); B. Delcourt *et al.*, Phys. Lett. B **29**, 75 (1969); S. A. Dytman *et al.*, Bull. Am. Phys. Soc. **35**, 1679 (1990).
- [5] H. Herminghaus, in *Proceedings of the 1990 Linear Accelerator Conference, Albuquerque, NM, 1990* (Los Alamos National Laboratory, Los Alamos, 1991).
- [6] I. Anthony *et al.*, Nucl. Instrum. Methods Phys. Res., Sect. A **301**, 230 (1991).
- [7] R. Novotny, IEEE Trans. Nucl. Science **38**, 379 (1991).
- [8] A. R. Gabler *et al.*, Nucl. Instrum. Methods Phys. Res., Sect. A **346**, 168 (1994).
- [9] B. Krusche, in *Proceedings of the II TAPS Workshop, Guardamar, 1993*, edited by J. Diaz and Y. Schutz (World Scientific, Singapore, 1993).
- [10] B. Krusche *et al.*, Z. Phys. A (to be published).
- [11] R. Brun *et al.*, CERN Report No. GEANT3 Cern/DD/ee/84-1, 1986.
- [12] H. R. Hicks *et al.*, Phys. Rev. D **7**, 2614 (1973).
- [13] L. Montanet *et al.*, Phys. Rev. D **50**, 1173 (1994) (Review of Particle Properties).
- [14] S. Homma *et al.*, J. Phys. Soc. Jpn. **57**, 828 (1988).